

Thermodynamics and holographic entanglement entropy for spherical black holes in 5D Gauss-Bonnet gravity

Yuan Sun,¹ Hao Xu,² Liu Zhao³

School of Physics, Nankai University, Tianjin 300071, China

E-mail: sunyuan14@mail.nankai.edu.cn, haoxu@mail.nankai.edu.cn,
lzhao@nankai.edu.cn

ABSTRACT: The holographic entanglement entropy is studied numerically in (4+1)-dimensional spherically symmetric Gauss-Bonnet AdS black hole spacetime with compact boundary. On the bulk side the black hole spacetime undergoes a van der Waals-like phase transition in the extended phase space, which is reviewed with emphasis on the behavior on the temperature-entropy plane. On the boundary, we calculated the regularized HEE of a disk region of different sizes. We find strong numerical evidence for the failure of equal area law for isobaric curves on the temperature-HEE plane and for the correctness of first law of entanglement entropy, and briefly give an explanation for why the latter may serve as a reason for the former, i.e. the failure of equal area law on the temperature-HEE plane.

Contents

1	Introduction	1
2	Thermodynamics for Gauss-Bonnet AdS Black holes	2
3	HEE in Gauss-Bonnet AdS gravity	5
4	Numerical results	7
5	Concluding remarks	12

1 Introduction

The gauge-gravity duality [1] is a promising way to make a connection between general relativity and quantum field theory. According to AdS/CFT correspondence, the black holes in AdS spacetime are dual to strongly-coupled large N gauge theories at finite temperature. The thermodynamics of black hole predicts phase transition in AdS spacetime, such as the Hawking-Page phase transition in Schwarzschild-AdS spacetime [2], which can be explained as the gravitational dual of QCD confinement/deconfinement transition [3, 4]. Black thermodynamics is also studied for charged black holes, and a first order phase transition was found in Reissner-Nordström AdS (RN AdS) spacetime [5, 6].

Recently, this analogy is extended to more general cases. By identifying the negative cosmological constant as an effective pressure $P = -\frac{\Lambda}{8\pi}$, the thermodynamics of black hole can be established on the extended phase space [7, 8]. The physical meaning of the thermodynamical volume that is conjugate to the effective pressure P remains to be fully understood, but it is conjectured to satisfy the reverse isoperimetric inequality [9]. In this consideration, the black hole mass is taken as the enthalpy H rather than the internal energy. The extended phase space thermodynamics has been investigated for many different spacetimes [10–28], and in many cases the extended phase space thermodynamic behavior is very similar to van der Waals liquid-gas system.

Up to now the dual field theory interpretation of the van der Waals-like phase transition remains unknown. However, progress has been made in this direction recently. In Ref. [29], it was found that the holographic entanglement entropy (HEE) as a function of temperature behaves qualitatively the same as black hole entropy in the context of a charged black hole in AdS background with finite volume. In this case, the HEE undergoes van der Waals-like phase transitions, and an inflexion point appears on the temperature-HEE curve at the same critical temperature. More recently, the similarity between the two kinds of entropies has been investigated further by considering Maxwell's equal area law, which holds for black hole entropy, and seems to be still valid on the HEE-temperature curve [30]. The numerical

results show that for RN-AdS black holes this “equal area law” on the HEE-temperature curve holds up to an accuracy of around 1%, however, it fails for dyonic RN-AdS black holes. Therefore, to get a better understanding of the field theory interpretation of the van der Waals-like phase transitions, it is important to examine whether these ideas applies to other gravity models. This connection has been extended to other cases [31–34], including the extended phase space. It seems that the HEE can be a nice probe of the extended phase space.

Motivated by the above considerations and progresses, we extended the study of van der Waals-like behavior for HEE to Gauss-Bonnet AdS black holes with a spherical horizon in (4+1)-dimensions. The thermodynamics of this particular black hole spacetime has been studied in the extended phase space in [14]. It was shown that for GB-AdS black holes, the $P - V$ criticality and phase transition only occurs when the black hole has a spherical horizon. When the charge of the black hole is turned off, only in (4+1)-dimension the $P - V$ criticality and phase transition takes place.

The inclusion of Gauss-Bonnet term is a non-trivial generalization of Einstein gravity. As a consequence, one must employ the HEE formula for general higher derivative gravity [35–38]. We will show that that the equal area law on the temperature-HEE plane fails but a van de Waals-like behavior on both the temperature-HEE and the temperature-black hole mass curves indeed holds.

The rest of the paper is organized as follows: in section 2, we review the black hole thermodynamics for spherically symmetric GB-AdS black holes, and discuss the critical behavior and Maxwell equal area law on the entropy-temperature plane. In section 3, we briefly review the holographic entanglement entropy in Gauss-Bonnet gravity and present the HEE formula for our setup. In section 4, The numerical results are presented, which include, in particular, the numerical evidence for the failure of the equal area law on the temperature-HEE plane and the correctness of the first law of entanglement entropy, which has never been established before. By employing the linear relationship between HEE and black hole mass, we give an explanation for why the equal area law fails on the the temperature-HEE plane. In the final section, we present some concluding remarks.

2 Thermodynamics for Gauss-Bonnet AdS Black holes

In this section, we give a brief review of the thermodynamics of Gauss-Bonnet AdS Black holes. The detailed calculation can be found in [14, 39, 40]. The action of Gauss-Bonnet gravity in $(d + 1)$ dimensions can be written as [39]

$$\mathcal{I} = \frac{1}{16\pi G} \int d^{d+1}x \sqrt{-g} [R - 2\Lambda + \alpha_{GB} \mathcal{L}_{GB}] \quad (2.1)$$

where α_{GB} is the Gauss-Bonnet coefficient and

$$\mathcal{L}_{GB} = R^2 - 4R_{ab}R^{ab} + R_{abcd}R^{abcd} \quad (2.2)$$

is known as Gauss-Bonnet density. The Gauss-Bonnet coefficient can be identified with the inverse string tension with positive value in string theory, so we shall only consider the case

$\alpha_{GB} > 0$ in this paper. For later convenience, we reparametrize the negative cosmological constant as $\Lambda = -d(d-1)/(2L^2)$ and the Gauss-Bonnet coefficient as $\alpha = \alpha_{GB}(d-2)(d-3)$.

Gauss-Bonnet gravity admits pure AdS solution with Riemann tensor $R_{abcd} = -(g_{ca}g_{bd} - g_{cb}g_{ad})/\tilde{L}^2$ and the radius \tilde{L} is given by

$$\tilde{L}^2 = \frac{2\alpha}{1 - \sqrt{1 - \frac{4\alpha}{L^2}}}. \quad (2.3)$$

It follows that the Gauss-Bonnet coefficient must satisfy $\alpha \leq L^2/4$ in order that the pure AdS solution exists. Besides, there exists another constraint by demanding the causality of dual field theory [41]

$$-\frac{(3d+2)(d-2)}{4(d+2)^2}L^2 \leq \alpha \leq \frac{(d-2)(d-3)(d^2-d+6)}{4(d^2-3d+6)^2}L^2. \quad (2.4)$$

In this paper, we will be interested in the AdS black hole solutions which takes the form [14, 39, 42–46]

$$ds_{(d+1)}^2 = -f_{(d+1)}(r)dt^2 + \frac{1}{f_{(d+1)}(r)}dr^2 + r^2 h_{ij}dx^i dx^j, \quad (2.5)$$

where

$$f_{(d+1)}(r) = k + \frac{r^2}{2\alpha} \left(1 \pm \sqrt{1 + \frac{64\pi G\alpha M}{(d-1)\Sigma_k r^d} - \frac{4\alpha}{L^2}} \right), \quad (2.6)$$

h_{ij} is the metric on the $(d-1)$ -dimensional hypersurface with constant curvature $(d-1)(d-2)k$ and volume Σ_k with $k = -1, 0, 1$, M is black hole mass. Among the two branches of solutions, only the “ $-$ ” branch is ghost free, so we shall only consider this case in this work. Moreover, we shall restrict ourselves only to the spherically symmetric case by taking $k = 1$.

In AdS background, the black hole event horizon r_+ is the largest root of $f_{(d+1)}(r)$. The enthalpy and temperature can be obtained by using two equations $f_{(d+1)}(r_+) = 0$ and $T = \frac{f'_{(d+1)}(r_+)}{4\pi}$, which yield

$$H \equiv M = \frac{(d-1)\Sigma_1 r_+^{d-2}}{16\pi} \left(1 + \frac{\alpha}{r_+^2} + \frac{16\pi P r_+^2}{d(d-1)} \right), \quad (2.7)$$

$$T = \frac{16\pi P r_+^4 / (d-1) + (d-2)r_+^2 + (d-4)\alpha}{4\pi r_+ (r_+^2 + 2\alpha)}, \quad (2.8)$$

where the pressure P is defined as $P = -\frac{\Lambda}{8\pi}$.

The black hole entropy [39] and thermodynamic volume can also be easily calculated

$$S = \frac{\Sigma_1 r_+^{d-1}}{4} \left[1 + \frac{2(d-1)\alpha}{(d-3)r_+^2} \right], \quad (2.9)$$

$$V = \left(\frac{\partial H}{\partial P} \right)_S = \frac{\Sigma_1 r_+^d}{d}. \quad (2.10)$$

These quantities satisfy the first law of black hole thermodynamics in the extended phase space [40], i.e.

$$dH = TdS + VdP, \quad (2.11)$$

or, in terms of Gibbs free energy $G(T, P) = H - TS$,

$$dG = VdP - SdT. \quad (2.12)$$

As discussed in [14], there exists some $P - V$ critical behavior and first-order phase transition in this extended phase space in $d + 1 = 5$ dimensions, which is similar to the van der Waals liquid-gas system. One can perform similar analysis on the $T - S$ plane by fixing P in eq.(2.12). The critical point can be determined by solving following two equations

$$\left(\frac{\partial T}{\partial S}\right)_P = 0, \quad \left(\frac{\partial^2 T}{\partial S^2}\right)_P = 0. \quad (2.13)$$

For ease of the forthcoming numerical calculations, we set $\alpha = 1, \Sigma_1 = 1$ in the rest of the paper. Then the above equations give rise to the following critical pressure and critical radius for the black hole,

$$P_c = \frac{1}{48\pi}, \quad r_c = \sqrt{6}. \quad (2.14)$$

The corresponding critical temperature is then

$$T_c = \frac{\sqrt{6}}{12\pi}. \quad (2.15)$$

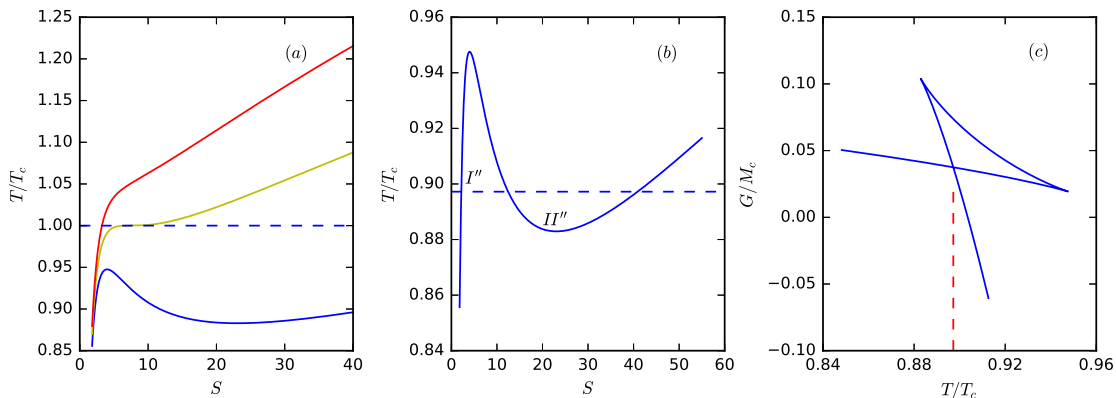


Figure 1. (a) Isobaric curves on (4+1)-dimensional Gauss-Bonnet AdS black hole with different pressure. From bottom to top the corresponding pressure are $0.7P_c$ (blue), P_c (orange), $1.2P_c$ (red). The dashed horizontal line(green) located at $T = T_c$. (b) Zoom in of the $P = 0.7P_c$ (blue) curve in (a). The dashed horizontal line corresponds to $T = T^*$. (c) Gibbs free energy along the isobaric curve in (b), The dashed vertical line corresponds to $T = T^*$.

In Ref. [40], the Maxwell's equal area law for Gauss-Bonnet AdS black holes is studied on the $P - V$ plane. In the following we shall reconstruct it on the $T - S$ plane. Fig.1(a)

gives the isobaric curves on the $T-S$ plane at pressures $P = 0.7P_c, P_c, 1.2P_c$ are presented. It can be seen that, when P is lower than the critical pressure P_c , there may exist three black holes of different sizes at the same temperature. However, the medium sized black hole is unstable since its heat capacity $C = T(\partial S/\partial T)$ is negative. Naturally, one wishes to know how Gibbs free energy varies along the isobaric curve. As is shown in Fig.1(c), there is an intersection point at $T = T^* < T_c$ on the isobaric Gibbs free energy versus temperature curve, which implies that at this temperature the small black hole may jump into a large black hole. This is a first order phase transition similar to the phase transition studied in the $P-V$ plane. The value of T^* can be determined by the Maxwell's equal area law since the Gibbs free energy remains unchanged during the phase transition. By referring to the closed regions formed by the isobaric $T-S$ curve and the isotherm $T = T^*$ as I'' and II'' (see Fig.1(b)), the equal area law can be expressed symbolically as

$$A(I'') = A(II''), \quad (2.16)$$

where

$$A(I'') \equiv \int_{S_1}^{S_3} |T(S) - T^*| dS, \quad A(II'') \equiv \int_{S_3}^{S_2} |T(S) - T^*| dS,$$

S_1 , S_2 and S_3 are respectively the smallest, largest and the intermedium solution of the equation $T(S) = T^*$. Equivalently, we can also re-express (2.16) as

$$A_L \equiv T^*(S_2 - S_1) = \int_{S_1}^{S_2} T(S) dS \equiv A_R. \quad (2.17)$$

However, when calculating the relative disagreements between the areas of the two closed regions, one should avoid using this latter expression, because neither A_L nor A_R corresponds to the area of any of the closed regions.

When $P = P_c$, there is an inflection point on the isobaric curve, and the area of both closed regions mentioned shrinks to zero. In this case, the size of the three black holes at the same temperature becomes identical, and the phase transition becomes continuous and is of the second order. If the pressure P increases further so that $P > P_c$ holds, T becomes a monotonous function of S , and there can be only a single black hole at each temperature, therefore the phase transition no longer occurs.

3 HEE in Gauss-Bonnet AdS gravity

Nowadays much attention has been focused on the research of entanglement entropy, which appears in many fields of physics, such as quantum field theory[47, 48], condensed matter physics[49], and quantum information[50]. For a quantum system with density matrix ρ , the entanglement entropy of a subsystem A is defined as

$$S_A = -\text{Tr} \rho_A \ln \rho_A, \quad (3.1)$$

where ρ_A is the reduced density matrix of A , which is defined by tracing over the degrees of freedom in the complementary subsystem \bar{A} of A , i.e.

$$\rho_A = \text{Tr}_{\bar{A}} \rho. \quad (3.2)$$

In the framework of AdS/CFT, Ryu and Takayanagi conjectured that the entanglement entropy of the dual field theory can be calculated holographically from the gravity side [51, 52] using the formula

$$S_A = \frac{\text{Area}(\Sigma)}{4G}, \quad (3.3)$$

where Σ is the co-dimension 2 minimal surface whose boundary coincides with the entangling surface between A and \bar{A} , and G is the Newton constant of the bulk theory. This formula applies to Einstein gravity. This geometric description is reminiscent of the Bekenstein-Hawking entropy for black holes since both are proportional to the area of some surfaces. Moreover, the similarity between the two kinds of entropies can go beyond Einstein gravity [38]. For Lovelock gravity the holographic entanglement entropy is calculated by minimizing a certain surface functional which is originally used to compute black hole entropy in Lovelock gravity [53] (this surface functional is denoted as S_{JM} in [38]). The general formula for HEE in higher curvature gravity is given in [36, 37], which is based on the generalized gravitational entropy introduced in [35]. For Gauss-Bonnet gravity the holographic entanglement entropy takes the form [36, 38]

$$S_A = \frac{1}{4G} \int_{\Sigma} d^{d-1}x \sqrt{h} (1 + \alpha R) + \frac{\alpha}{2G} \int_{\partial\Sigma} K, \quad (3.4)$$

where K is the trace of the extrinsic curvature of Σ and R is intrinsic curvature of Σ . Note, however, that in previous studies, the dual field theory lives on a flat d -dimensional boundary, and what we would like to study in the following is the case when the dual theory lives on a d -dimensional spacetime with compact spatial section.

To be more specific, we shall restrict ourselves to the spherically symmetric (i.e. $k = 1$) (4+1)-dimensional GB-AdS black hole spacetime with line element

$$ds^2 = -f_{(5)}(r) dt^2 + \frac{dr^2}{f_{(5)}(r)} + r^2 (d\theta^2 + \sin^2 \theta (d\varphi^2 + \sin^2 \varphi d\omega^2)). \quad (3.5)$$

The subsystem A is a subset on the boundary of the bulk spacetime at $r = r_0$ (here r_0 plays the role of UV cutoff) and is chosen to have a spherical boundary S^2 which plays the role of entangling surface. Therefore, in coordinates as used in (3.5), the entangling surface can be parameterized as a constant θ hypersurface $\theta = \theta_0$ with coordinates $0 \leq \varphi \leq \pi$, $0 \leq \omega < 2\pi$. Let us remark that, in principle, the boundary of the bulk spacetime should be taken at $r = \infty$. However, setting $r = \infty$ directly in the metric would effectively remove the M dependence and meanwhile render most of the metric components divergent. Therefore taking an appropriate UV cutoff at $r = r_0$ is a usual practice.

Because of the spherical symmetries, the radial coordinates at any point on Σ depends only on θ but not on φ and ω . Therefore, the induced metric on Σ can be written as

$$h_{ab} dx^a dx^b = \left(\frac{1}{f_{(5)}(r(\theta))} r'^2(\theta) + r^2(\theta) \right) d\theta^2 + r(\theta)^2 \sin^2 \theta d\Omega^2, \quad (3.6)$$

where the prime denotes the derivative with respect to θ and $d\Omega^2$ is the line element on a unit two-sphere. The scalar curvature of Σ can be calculated as

$$R = 2e^{-2F} - 4\nabla^2 F - 6(\partial F)^2, \quad (3.7)$$

where

$$e^{2F} = r^2(\theta) \sin^2 \theta, \quad \nabla^2 F = \frac{1}{\sqrt{h_{\theta\theta}}} \partial_\theta (\sqrt{h_{\theta\theta}} h^{\theta\theta} \partial_\theta F), \quad (\partial F)^2 = h^{\theta\theta} (\partial_\theta F)^2. \quad (3.8)$$

To obtain the extrinsic curvature K , we define the outward pointing normal vector at $\partial\Sigma$:

$$n_a = \sqrt{h_{\theta\theta}} \delta_{\theta a}, \quad n^a = \sqrt{h^{\theta\theta}} \delta_{\theta a}. \quad (3.9)$$

Using this normal vector, the extrinsic curvature K on $\partial\Sigma$ is defined as

$$K = (h^{ab} - n^a n^b) \nabla_a n_b. \quad (3.10)$$

Combining the above data, the HEE formula Eq.(3.4) for the subsystem A can be rearranged into

$$S_A = \pi \int_0^{\theta_0} d\theta \left[\left(\frac{r'^2}{f_{(5)}} + r^2 \right)^{1/2} (2\alpha + r^2 \sin^2 \theta) + 2\alpha \left(\frac{r'^2}{f_{(5)}} + r^2 \right)^{-1/2} (r \cos \theta + r' \sin \theta)^2 \right], \quad (3.11)$$

which is to be minimized and integrated out. Notice that we have set the Newton constant $G = 1$ in the last formula.

The minimization of S_A involves a variational process which yields a very complicated second order differential equation for the function $r(\theta)$. This differential equation should then be solved using the boundary conditions

$$r'(0) = 0, \quad r(\theta_0) = r_0 \quad (3.12)$$

and then be substituted back into (3.11) to get the final result. However, as r_0 approaches infinity, the direct evaluation of S_A will become divergence. Thus a regularization by subtracting the entanglement entropy corresponding to the “zero mass black hole” (i.e. pure AdS background) is necessary. The outcome of the combined operations as described above will be the regularized HEE

$$\delta S = S_A - S_A|_{M=0}. \quad (3.13)$$

Due to the overwhelming complicatedness of the related differential equation, the only way to work out the above process is to resort to numerical methods.

4 Numerical results

In this section, we shall study the temperature vs regularized HEE relationship using numerical method. For RN-AdS [30] and massive gravity [32], the $T - \delta S$ curve was shown to possess van der Waals-like behavior at $T < T_c$, and it was conjectured that an equal area law might also hold on the $T - \delta S$ plane because numerical calculations show that the relative disagreement between the area of the two closed regions formed by the $T - \delta S$ curve

and the $T = T^*$ line is as small as 1%, where T^* is the same phase equilibrium temperature in the corresponding extended phase space thermodynamics of the black hole spacetime. Now we would like to see whether similar van der Waals behavior and/or the equal areal law appears in the situation of spherical GB-AdS black hole spacetime.

We shall still focus on the $(4 + 1)$ -dimensional case. Within the parameter region $0.7 < T/T_c < 1.3$, $0.7 < P/P_c < 1.3$, the numerical value of the radius r_+ of the event horizon of the spherical GB-AdS black hole can be shown to be less than 10. Thus we set $r_0 = 300$, which is large enough as compared to the radius of the event horizon.

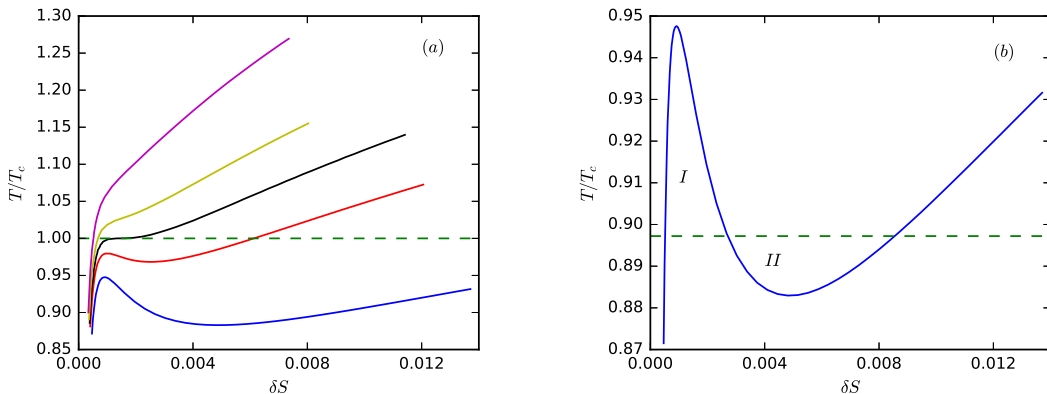


Figure 2. $T - \delta S$ curves at $\theta_0 = 0.1$. (a) From bottom to top, the pressures corresponding to each curve are: $0.7P_c$, $0.9P_c$, P_c , $1.1P_c$ and $1.3P_c$. The dashed horizontal line is located at $T = T_c$. (b) Zoom in of the $P = 0.7P_c$ curve in (a). The dashed horizontal line corresponds to $T = T^*$.

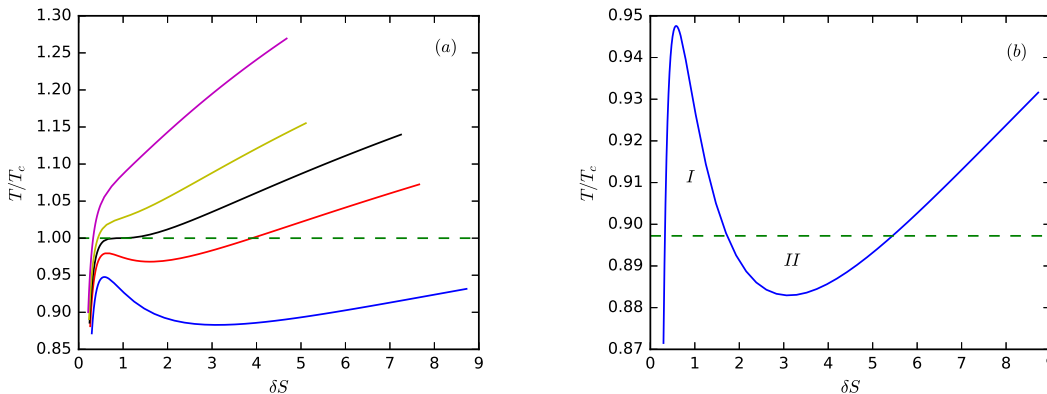


Figure 3. $T - \delta S$ plots at $\theta_0 = 0.5$. (a) From bottom to top, the pressures are: $0.7P_c$, $0.9P_c$, P_c , $1.1P_c$ and $1.3P_c$. The dashed horizontal line corresponds to $T = T_c$. (b) Zoom in of the $P = 0.7P_c$ curve in (a). The dashed horizontal line corresponds to $T = T^*$.

In Fig.2 and Fig.3, we present the plots of temperature versus regularized HEE δS at several fixed pressures. These two figures corresponds to different sizes of the entanglement

surface characterized by $\theta_0 = 0.1$ and $\theta_0 = 0.5$ respectively. It can be seen that, when the pressure is lower than the critical pressure P_c , there can be three different δS if the temperature takes value in a certain range. As P approaches P_c from below, the three different values of δS move closer, until they merge into a single value at $P = P_c$. When $P > P_c$, T becomes monotonic in δS . Such behavior is qualitatively similar to the temperature versus black hole entropy curves as shown in Fig.1.

Next we would like to examine whether there is an equal area law on the $T - \delta S$ plane. The two closed regions I and II formed by the $T - \delta S$ curve and the horizontal line $T = T^*$ are explicitly marked in Fig.2(b) and Fig.3(b) for the cases $\theta_0 = 0.1$ and $\theta_0 = 0.5$ respectively. The phase equilibrium temperature T^* , the areas of both closed regions and their relative disagreement are presented numerically at the given pressures $P/P_c = 0.6, 0.7, 0.8, 0.9$ respectively in Table 1 and Table 2. It can be seen from these tables that, as the pressure approaches P_c from below, the relative disagreement between the areas of the two closed regions decreases. However, at lower pressures, the relative disagreement can become significantly large, and consequently the equal area law cannot hold on the $T - \delta S$ plane.

P/P_c	T^*/T_c	A(I)	A(II)	(A(I)-A(II))/A(I)
0.6	0.8485	1.2490×10^{-4}	1.1468×10^{-4}	8.18%
0.7	0.8972	5.7431×10^{-5}	5.4452×10^{-5}	5.12%
0.8	0.9381	2.1475×10^{-5}	2.0790×10^{-5}	3.19%
0.9	0.9721	4.5825×10^{-6}	4.5162×10^{-6}	1.45%

Table 1. Areas and their relative disagreement for the regions I and II at $\theta_0 = 0.1$.

P/P_c	T^*/T_c	A(I)	A(II)	(A(I)-A(II))/A(I)
0.6	0.8485	7.9775×10^{-2}	7.3208×10^{-2}	8.25%
0.7	0.8972	3.6551×10^{-2}	3.4670×10^{-2}	5.14%
0.8	0.9381	1.3582×10^{-2}	1.3229×10^{-2}	2.59%
0.9	0.9721	2.9091×10^{-3}	2.8782×10^{-3}	1.06%

Table 2. Areas and their relative disagreement for the regions I and II at $\theta_0 = 0.5$.

Although we presented the numerical results only for two distinct values of $\theta_0 = 0.1, 0.5$, this does not imply that these values of θ_0 are special in any sense. Actually we have carried out the numerical process for some other values of θ_0 , and the results are qualitatively the same. Therefore we conclude that the break down of equal area law on the $T - \delta S$ plane should be a generic phenomenon for the HEE associated with the spherically symmetric GB-AdS black hole spacetime.

Besides the qualitative $T - \delta S$ behavior, let us examine another important aspect of HEE in the case of spherically symmetric GB-AdS black holes, i.e. the so-called entanglement thermodynamics. In Ref. [54] (see also [55]), the first law of entanglement entropy has been proposed, which states that the increase of HEE is proportional to the increase of

the energy of the subsystem, i.e. $\delta S \propto \Delta E_A$, provided $ml^d \ll 1$, where m is proportional to the black hole mass and l is related to the size of the subsystem A which is of the order $z = z_*$ in $d = 4$ (z_* is the Poincare radial coordinate which marks the position of the codimension 2 hypersurface). In our convention, we have $r \sim 1/z$ and so the above condition becomes $\frac{M}{r(0)^d} \ll 1$ (we still take $d = 4$). It should be noted that the calculation in [54] was performed in spacetime with planar boundary in contrast to the compact boundary in our case. Therefore, it is interesting to see whether the first law of entanglement entropy still holds in our case. It should be remarked that the increase ΔE_A of the subsystem A of the dual field theory is proportional to the black hole mass M [55, 56], therefore what we would like to explore is whether there is a linear relationship between the regularized HEE δS and the black hole mass M .

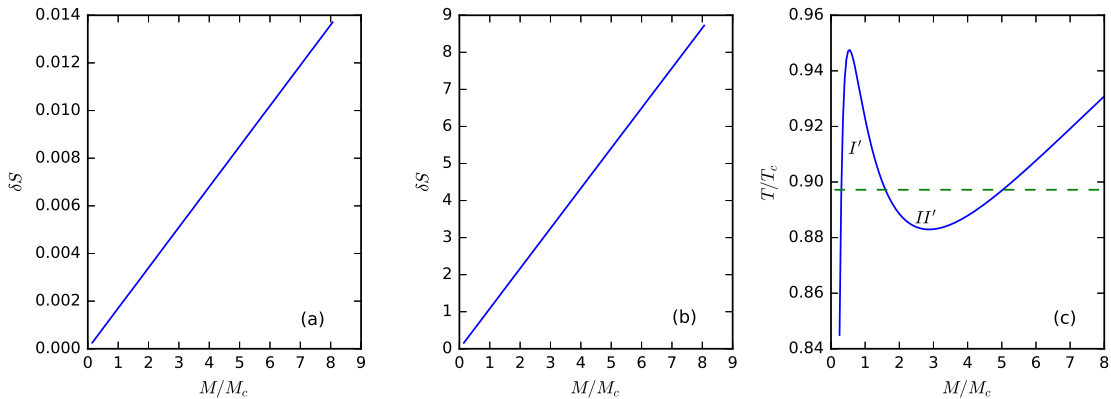


Figure 4. δS and T versus M at $P = 0.7P_c$. (a) δS vs M with $\theta_0 = 0.1$; (b) δS vs M with $\theta_0 = 0.5$. (c) T vs M , the dashed horizontal line corresponds to $T = T^* \simeq 0.8972 T_c$. The two closed regions are marked as I' and II' respectively.

Fig.4(a) and Fig. 4(b) give the plot of δS as function of M at the fixed pressure $P/P_c = 0.7$ in the cases of $\theta_0 = 0.1$ and $\theta_0 = 0.5$ respectively. It turns out that for both small and large subsystem A , there is a very good linear relationship between δS and the black hole mass M . In fact, this linear relationship shows up under all parameter ranges as presented in Tables 1 and 2. This indicates that the first law of entanglement entropy indeed holds in our case.

P/P_c	T^*/T_c	$A(I')$	$A(II')$	$(A(I')-A(II'))/A(I')$
0.6	0.8485	6.8084×10^{-2}	6.2521×10^{-2}	8.17%
0.7	0.8972	3.3759×10^{-2}	3.2034×10^{-2}	5.11%
0.8	0.9381	1.3451×10^{-2}	1.3090×10^{-2}	2.68%
0.9	0.9721	3.0562×10^{-3}	3.0282×10^{-3}	0.91%

Table 3. Areas and their relative disagreement for the regions I' and II' on $T - M$ plane.

Now since δS is proportional to M , one naturally expects that the $T - M$ relationship

must be qualitatively similar to the $T - \delta S$ relationship. A little calculation indicates that

$$\left(\frac{\partial T}{\partial M}\right)_P = \left(\frac{\partial T}{\partial S}\right)_P \left(\frac{\partial S}{\partial M}\right)_P = 0, \quad (4.1)$$

$$\left(\frac{\partial^2 T}{\partial M^2}\right)_P = \left(\frac{\partial T}{\partial S}\right)_P \left(\frac{\partial^2 S}{\partial M^2}\right)_P + \left(\frac{\partial^2 T}{\partial S^2}\right)_P \left(\frac{\partial S}{\partial M}\right)_P^2 = 0, \quad (4.2)$$

where the last equality holds at the critical point on the $T - S$ plane, thanks to Eq.(2.13). Exploring the expressions (2.7) and (2.8), one can show that there is an oscillatory segment on each $T - M$ curve if $P < P_c$. Furthermore, comparing the areas of the closed regions I' and region II' in in Fig.4(c), we find that the relative disagreements are roughly of the same order as in the cases of the $T - \delta S$ curves. For detailed numerical results, see Table 3.

It should be pointed out that there is no reason to think of the areas $A(I')$ and $A(II')$ as being equal in black hole thermodynamics. Therefore, the linear relationship between δS and M may serve as a good reason in judging that there is no equal area law on the $T - \delta S$ plots.

At this stage, it seems necessary to address the following problem: why the equal area law on the $T - \delta S$ plane seems to hold in the case of charged AdS black hole [30] whilst it is not the case for spherically symmetric Gauss-Bonnet black hole? To our understanding, this apparent controversy has nothing to do with the choice of gravity models. The seemingly holding equal area law in [30] is the consequence of the insufficient exploration on the range of the charge parameter Q (which plays similar role as the pressure P in the present work). In Fig.2 of [30], only the case $Q = 0.9Q_c$ had been checked numerically (however with several values of θ_0). Had we explored only the case $P = 0.9P_c$ in our work, one might draw the conclusion that the equal area law should also hold on the $T - \delta S$ plane for spherically symmetric Gauss-Bonnet black hole up to the relative disagreement around 1% (see the bottom rows of Tables 1 and 2). In fact, if one looks only at these bottom rows, the relative disagreements between the two closed areas are even smaller than that found in [30]. However, exploring broader ranges of the parameter P has revealed the fact that the equal area law does not hold actually.

Q/Q_c	T^*/T_c	A(I)	A(II)	(A(I)-A(II))/A(I)
0.6	1.0955	3.0415×10^{-5}	2.5353×10^{-5}	16.64%
0.7	1.0724	1.5835×10^{-5}	1.4180×10^{-5}	10.45%
0.8	1.0488	6.6235×10^{-6}	6.2605×10^{-6}	5.48%
0.9	1.0247	1.5817×10^{-6}	1.5528×10^{-6}	1.86%

Table 4. A check for the “equal area law” on the $T - \delta S$ plane for (3+1)D RN-AdS black hole with $\theta_0 = 0.1$ and $\theta_c = 0.099$. Q_c and T_c are the critical charge and critical temperature respectively whose value are presented in [30]. T^* is the RN-AdS black hole phase equilibrium temperature.

To support the above statements, we have re-worked out the numerics for the RN-AdS black hole. One thing to remark here is that [30] has used a different cutoff scheme, i.e. instead of introducing a UV cutoff over r as we do in this paper, the author of [30] has chosen to use a cutoff θ_c over the angular variable θ . Anyway, complying completely with

Q/Q_c	T^*/T_c	A(I')	A(II')	(A(I')-A(II'))/A(I')
0.6	1.09545	3.9449×10^{-3}	3.2885×10^{-3}	16.64%
0.7	1.07238	2.0538×10^{-3}	1.8393×10^{-3}	10.44%
0.8	1.04881	8.5909×10^{-4}	8.1203×10^{-4}	5.48%
0.9	1.02470	2.0515×10^{-4}	2.0134×10^{-4}	1.86%

Table 5. The case for RN-AdS black hole on the $T - M$ plane.

the conventions of [30], we obtained numerical results which fully support the statements given in the last paragraph. Table 4 contains the numerical results for the two closed areas on the $T - \delta S$ plane and their relative disagreements for (3+1)D RN-AdS black hole. For simplicity, we present the results only for $\theta_0 = 0.1$ and $\theta_c = 0.099$, the cases for other choices of θ_0 have also been checked and the results are qualitatively the same. The value of the charge parameter varies from $0.6 Q_c$ to $0.9 Q_c$, where the bottom row corresponds exactly to the same parameter set presented in the first row of Table 1 of [30] (A(I) and A(II) respectively are denoted A_1 and A_2 in [30])¹. Table 5 presents the parallel results on the $T - M$ plane. From the last two tables one can see that, if broader ranges for the parameter Q had been explored in [30], one would not have drawn the conclusion that the equal area law holds on the $T - \delta S$ plane (nor on the $T - M$ plane). The reason for the breakdown for the equal area law in the RN-AdS case can also be attributed to the linear relationship between δS and M , which has also been numerically checked to hold at very high accuracy.

5 Concluding remarks

In this work, we extended the study of analogy between black hole entropy and HEE to (4+1)-dimensional spherically symmetric Gauss-Bonnet AdS black hole spacetime. The thermodynamics of the black hole is reviewed, which emphasis on the behaviors on the $T - S$ plane. Then the regularized HEE δS against the black hole temperature is calculated numerically. The results show that the isobaric $T - \delta S$ curves behave qualitatively the same as the isobaric $T - S$ curve and exhibits van der Waals-like structure, however there is no reason to believe there is an analogy of equal area law on the $T - \delta S$ plane.

We also find that the regularized HEE δS is proportional to the black hole mass M , which may be understood as the first law of holographic entanglement entropy. Note that for a spacetime with compact boundary, the first law of holographic entanglement entropy has never been established before. The linear relation between δS and M may also serve as an explanation for the failure of equal area law on the $T - \delta S$ plane.

¹The numerical values for A(I) and A(II) in the bottom row of Table 4 are about 0.6% less than the values given in [30]. We suspect that this difference might be originated from the choice of different numerical integration algorithms. The numerical program which we use for producing the table is available upon request, just send us an e-mail.

Notes added

After the first version of this manuscript has appeared on arXiv, we have noticed the more recent work [57], which also studied the holographic entanglement entropy versus temperature relationship for the (charged) spherically symmetric Gauss-Bonnet black holes. There the authors claimed the correctness of the equal area law on the $T - \delta S$ plane. However, the areas compared in that paper are A_L and A_R defined in (2.17) (with S replaced by δS), rather than the correct A(I) and A(II) used in the present paper. The “relative error” between A_L and A_R differs from the relative disagreement between A(I) and A(II) by adding the whole area below the isotherm $T = T^*$ (which is a huge quantity as compared to the area of the closed region) in the denominator, this explains why the relative errors presented in [57] are so small.

Acknowledgments

We would like to Xiao-Xiong Zeng for helpful discussions on the numerical methods. The numerical calculations in this work are carried out using both Mathematica and the Anaconda Scientific Python Distribution, which yield perfect agreements. This work is supported by the National Natural Science Foundation of China under the grant No. 11575088.

References

- [1] J. M. Maldacena, “The Large N limit of superconformal field theories and supergravity,” Int. J. Theor. Phys. **38**, 1113 (1999) [Adv. Theor. Math. Phys. **2**, 231 (1998)] [hep-th/9711200].
- [2] S. Hawking and D. N. Page, *Thermodynamics of Black Holes in anti-De Sitter Space*, *Commun.Math.Phys.* **87** (1983) 577.
- [3] E. Witten, “Anti-de Sitter space and holography,” Adv. Theor. Math. Phys. **2**, 253 (1998) [hep-th/9802150].
- [4] E. Witten, “Anti-de Sitter space, thermal phase transition, and confinement in gauge theories,” Adv. Theor. Math. Phys. **2**, 505 (1998) [hep-th/9803131].
- [5] A. Chamblin, R. Emparan, C. Johnson, and R. Myers, “Charged AdS black holes and catastrophic holography,” *Phys.Rev.* **D60** (1999) 064018, [hep-th/9902170].
- [6] A. Chamblin, R. Emparan, C. V. Johnson and R. C. Myers, “Holography, thermodynamics and fluctuations of charged AdS black holes,” *Phys. Rev. D* **60**, 104026 (1999) [hep-th/9904197].
- [7] D. Kastor, S. Ray and J. Traschen, “Enthalpy and the Mechanics of AdS Black Holes,” *Class. Quant. Grav.* **26**, 195011 (2009) [arXiv:0904.2765 [hep-th]].
- [8] D. Kubiznak and R. B. Mann, “P-V criticality of charged AdS black holes,” *JHEP* **1207**, 033 (2012) [arXiv:1205.0559 [hep-th]].
- [9] M. Cvetič, G. W. Gibbons, D. Kubiznak and C. N. Pope, “Black Hole Enthalpy and an Entropy Inequality for the Thermodynamic Volume,” *Phys. Rev. D* **84**, 024037 (2011) [arXiv:1012.2888 [hep-th]].

- [10] M. B. J. Poshteh, B. Mirza and Z. Sherkatghanad, “Phase transition, critical behavior, and critical exponents of Myers-Perry black holes,” *Phys. Rev. D* **88**, 024005 (2013) [arXiv:1306.4516 [gr-qc]].
- [11] N. Altamirano, D. Kubiznak and R. B. Mann, “Reentrant Phase Transitions in Rotating AdS Black Holes,” *Phys. Rev. D* **88**, 101502 (2013) [arXiv:1306.5756 [hep-th]].
- [12] N. Altamirano, D. Kubiznak, R. B. Mann and Z. Sherkatghanad, “Thermodynamics of rotating black holes and black rings: phase transitions and thermodynamic volume,” *Class. Quant. Grav.* **31** (2014) 042001 [arXiv:1401.2586 [hep-th]].
- [13] S. -W. Wei and Y. -X. Liu, “Critical phenomena and thermodynamic geometry of charged Gauss-Bonnet AdS black holes,” *Phys. Rev. D* **87**, no. 4, 044014 (2013) [arXiv:1209.1707 [gr-qc]].
- [14] R. -G. Cai, L. -M. Cao, L. Li and R. -Q. Yang, “P-V criticality in the extended phase space of Gauss-Bonnet black holes in AdS space,” *JHEP* **1309**, 005 (2013) [arXiv:1306.6233 [gr-qc]].
- [15] D. -C. Zou, Y. Liu and B. Wang, “Critical behavior of charged Gauss-Bonnet AdS black holes in the grand canonical ensemble,” *Phys. Rev. D* **90**, no. 4, 044063 (2014) [arXiv:1404.5194 [hep-th]].
- [16] S. Gunasekaran, R. B. Mann and D. Kubiznak, “Extended phase space thermodynamics for charged and rotating black holes and Born-Infeld vacuum polarization,” *JHEP* **1211**, 110 (2012) [arXiv:1208.6251 [hep-th]].
- [17] D. -C. Zou, S. -J. Zhang and B. Wang, “Critical behavior of Born-Infeld AdS black holes in the extended phase space thermodynamics,” *Phys. Rev. D* **89**, 044002 (2014) [arXiv:1311.7299 [hep-th]].
- [18] C. V. Johnson, “Thermodynamic Volumes for AdS-Taub-NUT and AdS-Taub-Bolt,” *Class. Quant. Grav.* **31**, no. 23, 235003 (2014) [arXiv:1405.5941 [hep-th]].
- [19] C. V. Johnson, “The Extended Thermodynamic Phase Structure of Taub-NUT and Taub-Bolt,” *Class. Quant. Grav.* **31**, 225005 (2014) [arXiv:1406.4533 [hep-th]].
- [20] W. Xu, H. Xu and L. Zhao, “Gauss-Bonnet coupling constant as a free thermodynamical variable and the associated criticality,” *Eur. Phys. J. C* **74**, 2970 (2014) [arXiv:1311.3053 [gr-qc]].
- [21] H. Xu, W. Xu and L. Zhao, “Extended phase space thermodynamics for third order Lovelock black holes in diverse dimensions,” *Eur. Phys. J. C* **74**, no. 9, 3074 (2014) [arXiv:1405.4143 [gr-qc]].
- [22] W. Xu and L. Zhao, “Critical phenomena of static charged AdS black holes in conformal gravity,” *Phys. Lett. B* **736**, 214 (2014) [arXiv:1405.7665 [gr-qc]].
- [23] A. M. Frassino, D. Kubiznak, R. B. Mann and F. Simovic, “Multiple Reentrant Phase Transitions and Triple Points in Lovelock Thermodynamics,” *JHEP* **1409**, 080 (2014) [arXiv:1406.7015 [hep-th]].
- [24] B. P. Dolan, A. Kostouki, D. Kubiznak and R. B. Mann, “Isolated critical point from Lovelock gravity,” *Class. Quant. Grav.* **31**, no. 24, 242001 (2014) arXiv:1407.4783 [hep-th].
- [25] C. O. Lee, “The extended thermodynamic properties of Taub-AdS/CNUT/Bolt-AdS/CAdS spaces,” *Phys. Lett. B* **738**, 294 (2014) [arXiv:1408.2073 [hep-th]].

- [26] A. Rajagopal, D. Kubiznak and R. B. Mann, “Van der Waals black hole,” *Phys. Lett. B* **737**, 277 (2014) [arXiv:1408.1105 [gr-qc]].
- [27] A. M. Frassino, R. B. Mann and J. R. Mureika, “Lower-Dimensional Black Hole Chemistry,” *Phys. Rev. D* **92**, no. 12, 124069 (2015) [arXiv:1509.05481 [gr-qc]].
- [28] C. O. Lee, “The Extended Thermodynamic Properties of a topological Taub-NUT/Bolt-AdS spaces,” *Phys. Lett. B* **753**, 470 (2016) [arXiv:1510.06217 [gr-qc]].
- [29] C. V. Johnson, “Large N Phase Transitions, Finite Volume, and Entanglement Entropy,” *JHEP* **1403**, 047 (2014) [arXiv:1306.4955 [hep-th]].
- [30] P. H. Nguyen, “An equal area law for holographic entanglement entropy of the AdS-RN black hole,” *JHEP* **1512**, 139 (2015) [arXiv:1508.01955 [hep-th]].
- [31] E. Caceres, P. H. Nguyen and J. F. Pedraza, “Holographic entanglement entropy and the extended phase structure of STU black holes,” *JHEP* **1509**, 184 (2015) [arXiv:1507.06069 [hep-th]].
- [32] X. X. Zeng, H. Zhang and L. F. Li, “Phase transition of holographic entanglement entropy in massive gravity,” [arXiv:1511.00383 [gr-qc]].
- [33] X. X. Zeng and L. F. Li, “Van der Waals phase transition in the framework of holography,” arXiv:1512.08855 [hep-th].
- [34] A. Dey, S. Mahapatra and T. Sarkar, “Thermodynamics and Entanglement Entropy with Weyl Corrections,” arXiv:1512.07117 [hep-th].
- [35] A. Lewkowycz and J. Maldacena, “Generalized gravitational entropy,” *JHEP* **1308**, 090 (2013) [arXiv:1304.4926 [hep-th]].
- [36] X. Dong, “Holographic Entanglement Entropy for General Higher Derivative Gravity,” *JHEP* **1401**, 044 (2014) [arXiv:1310.5713 [hep-th]].
- [37] R. X. Miao and W. z. Guo, “Holographic Entanglement Entropy for the Most General Higher Derivative Gravity,” *JHEP* **1508**, 031 (2015) [arXiv:1411.5579 [hep-th]].
- [38] L. Y. Hung, R. C. Myers and M. Smolkin, “On Holographic Entanglement Entropy and Higher Curvature Gravity,” *JHEP* **1104**, 025 (2011) [arXiv:1101.5813 [hep-th]].
- [39] R. -G. Cai, “Gauss-Bonnet black holes in AdS spaces,” *Phys. Rev. D* **65**, 084014 (2002) [hep-th/0109133].
- [40] H. Xu and Z. M. Xu, “Maxwell’s equal area law for Lovelock Thermodynamics,” arXiv:1510.06557 [gr-qc].
- [41] X. Zeng and W. Liu, “Holographic thermalization in Gauss-Bonnet gravity,” *Phys. Lett. B* **726**, 481 (2013) [arXiv:1305.4841 [hep-th]].
- [42] D. G. Boulware and S. Deser, “String Generated Gravity Models,” *Phys. Rev. Lett.* **55**, 2656 (1985).
- [43] D. L. Wiltshire, “Spherically Symmetric Solutions Of Einstein-maxwell Theory With A Gauss-bonnet Term,” *Phys. Lett. B* **169**, 36 (1986).
- [44] M. Cvetic, S. i. Nojiri and S. D. Odintsov, “Black hole thermodynamics and negative entropy in de Sitter and anti-de Sitter Einstein-Gauss-Bonnet gravity,” *Nucl. Phys. B* **628**, 295 (2002) [hep-th/0112045].

- [45] G. Kofinas and R. Olea, “Vacuum energy in Einstein-Gauss-Bonnet AdS gravity,” *Phys. Rev. D* **74**, 084035 (2006) [hep-th/0606253].
- [46] D. Kastor, S. Ray and J. Traschen, “Mass and Free Energy of Lovelock Black Holes,” *Class. Quant. Grav.* **28**, 195022 (2011) [arXiv:1106.2764 [hep-th]].
- [47] P. Calabrese and J. L. Cardy, “Entanglement entropy and quantum field theory,” *J. Stat. Mech.* **0406**, P06002 (2004) [hep-th/0405152].
- [48] H. Casini and M. Huerta, “Entanglement entropy in free quantum field theory,” *J. Phys. A* **42**, 504007 (2009) [arXiv:0905.2562 [hep-th]].
- [49] L. Amico, R. Fazio, A. Osterloh and V. Vedral, “Entanglement in many-body systems,” *Rev. Mod. Phys.* **80**, 517 (2008) [quant-ph/0703044].
- [50] V. Vedral, “The role of relative entropy in quantum information theory,” *Rev. Mod. Phys.* **74**, 197 (2002) [quant-ph/0102094].
- [51] S. Ryu and T. Takayanagi, “Holographic derivation of entanglement entropy from AdS/CFT,” *Phys. Rev. Lett.* **96**, 181602 (2006) [hep-th/0603001].
- [52] S. Ryu and T. Takayanagi, “Aspects of Holographic Entanglement Entropy,” *JHEP* **0608**, 045 (2006) [hep-th/0605073].
- [53] T. Jacobson and R. C. Myers, “Black hole entropy and higher curvature interactions,” *Phys. Rev. Lett.* **70**, 3684 (1993) [hep-th/9305016].
- [54] J. Bhattacharya, M. Nozaki, T. Takayanagi and T. Ugajin, “Thermodynamical Property of Entanglement Entropy for Excited States,” *Phys. Rev. Lett.* **110**, no. 9, 091602 (2013) [arXiv:1212.1164].
- [55] W. z. Guo, S. He and J. Tao, “Note on Entanglement Temperature for Low Thermal Excited States in Higher Derivative Gravity,” *JHEP* **1308**, 050 (2013) [arXiv:1305.2682 [hep-th]].
- [56] V. Balasubramanian and P. Kraus, “A Stress tensor for Anti-de Sitter gravity,” *Commun. Math. Phys.* **208**, 413 (1999) [hep-th/9902121].
- [57] S. He, L. F. Li and X. X. Zeng, “Holographic Van der Waals-like phase transition in the Gauss-Bonnet gravity,” arXiv:1608.04208 [hep-th].